Inhibitory effects and molecular mechanism on mushroom tyrosinase by condensed tannins isolation from the fruit of Ziziphus jujuba Mill. var. spinosa (Bunge) Hu ex H. F. Chow

Wei Song, Lu-Lu Liu, Yuan-Jing Ren, Shu-Dong Wei, Hai-Bo Yang

PII: S0141-8130(20)34622-5

DOI: https://doi.org/10.1016/j.ijbiomac.2020.09.259

Reference: BIOMAC 16889

To appear in: *International Journal of Biological Macromolecules*

Received date: 11 July 2020

Revised date: 22 September 2020

Accepted date: 30 September 2020

Please cite this article as: W. Song, L.-L. Liu, Y.-J. Ren, et al., Inhibitory effects and molecular mechanism on mushroom tyrosinase by condensed tannins isolation from the fruit of Ziziphus jujuba Mill. var. spinosa (Bunge) Hu ex H. F. Chow, *International Journal of Biological Macromolecules* (2018), https://doi.org/10.1016/j.ijbiomac.2020.09.259

Inhibitory effects and molecular mechanism on mushroom tyrosinase by condensed tannins isolation from the fruit of *Ziziphus jujuba Mill. var. spinosa (Bunge) Hu ex H. F. Chow*

Wei Song [1], Lu-Lu Liu [2], Yuan-Jing Ren [2], Shu-Dong Wei [2*], Hai-Bo Yang [1,3*]

1 School of Life Science and Engineering, Henan University of Urban Construction, Pingdingshan, Henan 467044, China; songwei@hncj.edu.cn

2 College of Life Science, Yangtze University, Jingzhou, Hubei 434025, China; 2378970509@qq.com, 1060739982@qq.com

3 Forestry College, Henan Agricultural University, Zhengzhou, Henan 450000, China; 30110508@hncj.edu.cn

*Correspondence: 30110508@hncj.edu.cn; weishudong2005@126.com

Abstract: The structure of extracted condensed tannin (CT) from the fruit of Sour jujube （*Ziziphus jujuba Mill. var. spinosa (Bunge) Hu ex H. F. Chow*） and the molecular mechanisms by which CT inhibits the activity of mushroom tyrosinase were investigated. The structure of CT was characterized by high performance liquid chromatography electrospray ionization mass spectrometry, and matrix-assisted laser desorption/ionization time-of-flight mass spectrometry. The kinetic assays were used to detect inhibition effect, type and mechanism. UV scanning, fluorescence quenching, copper interacting, o-quinone interaction and molecular docking assays were also used to reveal the molecular mechanisms by which CT inhibit tyrosinase. The results showed the main structural units of CT contain afzelechin/epiafzelechin, catechin/epicatechin, and atechin/epicatechin. Kinetic analysis showed that CT inhibits both the monophenolase and diphenolase activities of tyrosinase and exhibits reversible, mixed type mechanism. The fruit CT interacts primarily with the copper ions and specific amino acid residue (Asn191, Thr203, Ala202, Ser206, Met201, His194, His54, Glu182 and Ile42) in the active site of tyrosinase to disturb oxidation of substrates by tyrosinase. These results suggested the sour jujube fruit is a potential natural source of tyrosinase inhibitors, and has a potential to be used in food preservation, whitening cosmetics.

Keywords: tyrosinase; Sour jujube; inhibitor; molecular mechanism

1. Introduction

Tyrosinase, also known as a copper oxidase, a key enzyme to melanin synthesis, catalyzes the hydroxylation of monophenol molecules to catechols, which is then oxidized to DOPA. Excessive accumulation of melanin in the body leads to freckles, chloasma, senile plaque, and other skin diseases[1]. In fruit and vegetable storage and transportation, abnormal amounts of melanin can cause fruits and vegetables to brown, decreasing their taste and nutritional value[2, 3]. Therefore, tyrosinase is closely tied to our daily lives, and controlling tyrosinase is becoming an increasingly important topic of study for agriculture, cosmetics, and drug therapy. Due to the ineffectiveness, side effects from prolonged pharmaceutical use, food health, and beauty industry usage, traditionally synthesized tyrosinase inhibitors are being rejected by more and more people. Meanwhile, due to the growing recognition that plant extracts are easily degradable, environmentally friendly, have non-toxic side effects, and a relatively affordable price, plant extracts with functional or active products are increasingly being favored [4-8]. Therefore, it is of great significance for the food and pharmaceutical industry to screen the anti- tyrosinase substances from natural products.

Sour jujube (*Ziziphus jujuba Mill. var. spinosa (Bunge) Hu ex H. F. Chow*) is a deciduous shrub or small tree with a high nutritional and medicinal value, contains a variety of bioactive substances, such as Sour jujube polysaccharide, flavonoids, saponins, triterpenoids, alkaloids, cAMP, CGMP[9-11]. Several substances of jujube kernel, a mature seed of dried jujube plants have been extracted[12-18]. However, there are few reports concerning the sour jujube fruit's bioactivities，in particular from the fruit's tannin. To fully understand and thus utilize the Sour jujube it is necessary to extract CT from the fruit and investigate their bioactivities for anti-tyrosinase.

The CT from natural plant extracts is a kind of polyphenol polymer polymerized by flavone-3-ol monomers including catechin, epicatechin, gallicatechin and epicatechin in a certain proportion[19, 20]. CT is widely found in the tube bundle of roots, bark,

leaves, flowers, fruit, and other organs with a large molecular weight of 1000-20000u and complex structure. Their chemical properties and biological activities vary greatly depending on their plant origin, monomer composition, polymerization degree, and molecular interaction[21-23]. Currently, tannins of different plant species, including Leucaena[24], pine needles[25], apple[26, 27], longan[28], showed good tyrosinase inhibition. Unfortunately, some reported natural tyrosinase inhibitors in-vivo use is restricted due to their insufficient tyrosinase inhibitory activity or the food safety regulations[29]. Thus, looking for more effective and safer tannins to serve as tyrosinase inhibitors is indeed feasible.

To the best of our knowledge, the possible effect of CT from Sour jujube fruit on tyrosinase activity has not been described so far. Therefore, in this study, we chose to isolate CT and identify its structure from Sour jujube's fruit. Moreover, CT's tyrosinase inhibitory activity and molecular mechanism were investigated. This research would provide scientific evidence for the utilization of the CT as antityrosinase agents. This study suggested that CT from Sour jujube fruit is a good tyrosinase inhibitor and has great potential for usage in fruit and vegetable preservation, medicine, and cosmetics fields.

2. Materials and Method

2.1 Reagents

Mushroom tyrosinase (3030 U/mg), 3,4-dihydroxyphenylalanine (L-DOPA) and HPLC standards were purchased from Sigma-Aldrich (St. Louis, MO, USA). All other reagents and solvents used were of analytical grade.

2.2 CT sample preparation

The young fruits (about 20 days after flowering) of Sour jujube were collected in Xiangyun Park, Pingdingshan City, Henan Province, and were subsequently washed and freeze-dried. The plant samples were ground to a powder and stored at -20℃. The dried fruit powder (20 g each) was extracted three times with 70% (v/v) acetone at room temperature, after which the acetone was removed by rotating evaporation at 38℃ The

water phase was extracted with petroleum ether and ethyl acetate three times. The crude extracts were dissolved with 50% methanol, and loaded onto the Sephadex LH-20 column (50 cm length × 4 cm i.d). The elution was run with a methanol (A)–water (B) gradient (50% A, each 500 mL) at a constant flowrate of 1 mL/min. The purified tannin liquid was freeze-dried and stored at -20℃. The content of CT was determined by the butanol–HCl method.

2.3 HPLC-ESI-MS and MALDI-TOF MS analysis

Reversed-phase HPLC-ESI-MS analysis was detected by Agilent series 1200 system(Agilent, USA). The determination of MALDI-TOF MS was carried out on the Burker Reflex III (Germany) with the nitrogen laser, and the laser wavelength were 337 nm. Procedures for HPLC-ESI-MS and MALDI-TOF MS were as described previously[30].

2.4 Enzyme assay

The monophenolase and diphenolase activities assays were performed as previously reported[30]. The range concentration of CT was 0-70 μg/mL. All experiments values were determined at 475 nm using a UV-Vis spectrophotometer (Genesys 10S, USA). The temperature of enzymatic reaction was controlled at 30 ℃, and water bath was used to maintain a constant temperature. To describe the mixed-type inhibition mechanism, the Lineweaver-Burk equation in double reciprocal form can be written as:

$$v = \frac{V_m \cdot [S]}{K_m(1+\frac{[\mathrm{I}]}{K_\mathrm{I}}) + [S] \cdot (1+\frac{[\mathrm{I}]}{K_\mathrm{IS}})}$$

v: Enzymatic reaction rate, Km: Michaelis constant, *Ki*: inhibition constant of inhibitor to free enzyme, *Kis*: inhibition constant of inhibitor on enzyme substrate complex (ES), [*S*] : substrate concentration, [I] : inhibitor concentration.

2.5 UV Scanning Study

The experiment was carried out as described by Jiménez-Atiénzar et al. The process of L-Tyr oxidation by tyrosinase was performed in the absence and presence of CT. The data were recorded every minute following the addition of L-Tyr and enzyme (16.67

μg/mL). The scanning wavelength was 200-800 nm.

2.6 Fluorescence Quenching

In this study, fluorescence spectra were measured on a fluorescence spectrophotometer (F4600, Hitachi, Japan). The measurement conditions were fluorescence emission wavelengths of 300−450 nm, excitation wavelengths of 290 nm, and slit widths set to 2.5 nm for both the excitation and emission monochromators. For the measurement of the enzyme-CT interactions, enzyme (40 μg/mL) in PBS in a final volume of 0.4 mL was titrated with CT (0, 50, 100, 150 and 200 μg/mL).

2.7 The Chelating Ability between Cu2+ and CT

To detect the interaction between CT and tyrosinase, the chelating ability between Cu2+ and CT was investigated. Data were acquired after the addition of the same volume of $CuCl_2$ each time using a UV-Vis spectrophotometer (Genesys 10S, USA). The absorption spectra were recorded between 240 and 600 nm. The reaction system (3 mL) contained 100 μL of sample (3 mg/mL) solution, 100 μL of copper sulfate solution with different concentrations (0, 20, 40, 60, 80 and 100 μM), and 2.8 mL of sodium phosphate buffer (50 mM, pH 6.8).

2.8 Generation of the dopaquinone in absence enzyme

These experiments were carried out as described by Espin and Wichers8. Briefly, L-DOPA (1 mg/ml) was oxidized by $NaIO_4$ (1 mg/mL), and the yield of dopaquinone was recorded using a UV-Vis spectrophotometer (Genesys 10S, USA) in the presence of varying concentrations of CT (50, 100 μg/mL). The scanning wavelength was 240-800 nm.

2.9 Molecular docking

The selection of molecular docking methods was mainly determined by the use of docking modules for drug design software. The X-ray structure of mushroom tyrosinase (LWX2, RCSB Protein Data Bank) was used as the initial protein model for molecular docking. We analyzed Dock with the commonly used software molecular operation environment 2010 (MOE), for docking screening using drugs. MOE-DOCK includes the following steps: (1) Import protein crystal structure, hydrogenation and charge up, and energy minimization. (2) Find the binding site of the protein crystal structure forms a Gauss contact surface around the binding site to make it a docking

pocket for proteins. (3) Small molecule structure processing, energy optimization and conformation generation. (4) Enter docking program.

3 3. Results

3.1 HPLC-ESI-MS Analysis

High-purity CT from Sour jujube fruits were obtained by organic solvent extraction and column chromatography. Reversed-phase HPLC-ESI-MS further clarified the chemical composition of the CT. The products of depolymerization were separated and identified by reversed-phase HPLC-ESI-MS. HPLC showed that CT from the fruit of Sour jujube was similar in basic structure, contain gallate catechin/epigallate catechin (GC/EGC) and catechin/epicatechin (C/EC), and have C/EC as the main unit (Fig. 1 a).

3.2 MALDI-TOF MS analysis

MALDI-TOF MS was used to further explain the structural diversity of CT in terms of the polymer structure. CT is a group of flavane-3 alcohol structure unit connections by 4-8 (B) or 4-6 C-C key polydisperse polymers and is connected by a C-C and a C-O-C key of the double bond to a lesser extent (A). As shown in Fig. 1 b, C/EC and GC/EGC were common in the Plant CT unit, with two hydroxyls in both C3 and C4 are, with C4 forming one more hydroxyl than C3, indicating that the molecular weight of C4 is 16 Da more than C3, with 288 Da for the C3, 304 Da for C4, while some CT was 272 Da such as afzelechin/afzelechin (AF/EAF). The mass spectrometry results in Fig. 1b indicate that CT from the trimer (m/z 940.55) to fourteen polymers (m/z 4229.21) distribution of adjacent poly had a fixed difference, 288 Da, 304 Da or 272 Da, showing that the main structural units of CT contain C/EC as well as GC/EGC, and some AF/EAF.

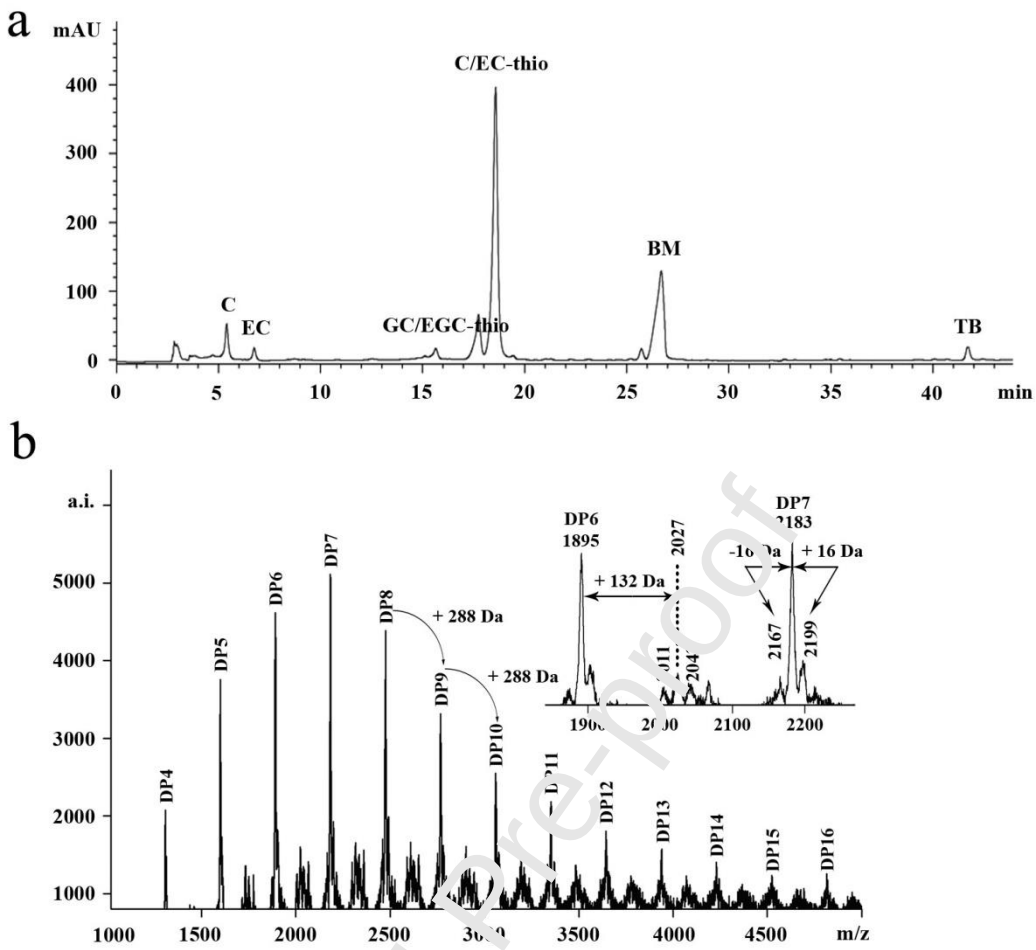

Figure 1. Structure characterization of the CT. (a) Reversed-phase HPLC–ESI-MS chromatograms. C/EC terminal unit catechin/epicatechin, C-thio/EC-thio and GC-thio/EGC-thio represented extender unit catechin/epicatechin and gallate catechin/epigallate catechin, respectively. BM represented benzyl mercaptan, TB represented Thiolytic byproduct (b) MALDI-TOF-MS spectra of the CT. DP degree of polymerization.

3.3 Detection of Inhibitory effect, mechanism and type

The reaction system uses L-Tyr as a substrate to detect the monophenolase activity in the presence of different concentrations of CT, which is used as the inhibitor. At the initial stage of the reaction, the product yield increases slowly and then becomes linear. The reaction system reaches a constant slope, which shows that the reaction is stable. The steady-state reaction rate of tyrosinase is equal to the slope of the line. The results show that in the presence of increasing amounts of CT, the steady-state rate was significantly decreased, indicating that CT can effectively reduce the monophenolase

activity in a dose-dependent manner (Fig. 2 a). The inhibitory concentration for the monophenolase activity decreased to 50% was 136.22 μg/mL.

The relationship between mushroom tyrosinase and CT is shown as Fig. 2 b. The results showed that L-DOPA was oxidized without lag time and that diphenolase activities were remarkably decreased in the presence of an increasing CT concentration. The concentration of inhibitors leading to half activity of enzyme was 57.67 μg/mL.

There was a set of straight lines that all passed through the origin (Fig. 2 c). With the concentration of CT increasing, the slope of line was decreased, indicating that the effect of CT on tyrosinase was reversible. As shown in Fig. 2 d, a set of straight lines intersects with the second quadrant. The Km values were extended, and the Vm values were reduced in the presence of increasing amounts of CT. We calculated the values of the inhibition constants (KI, 24.44 μg/mL) and of the enzyme−substrate complexes (KIS, 70.97 μg/mL) independently. KI< KIS and KIS is 2.9 times as large as KI.

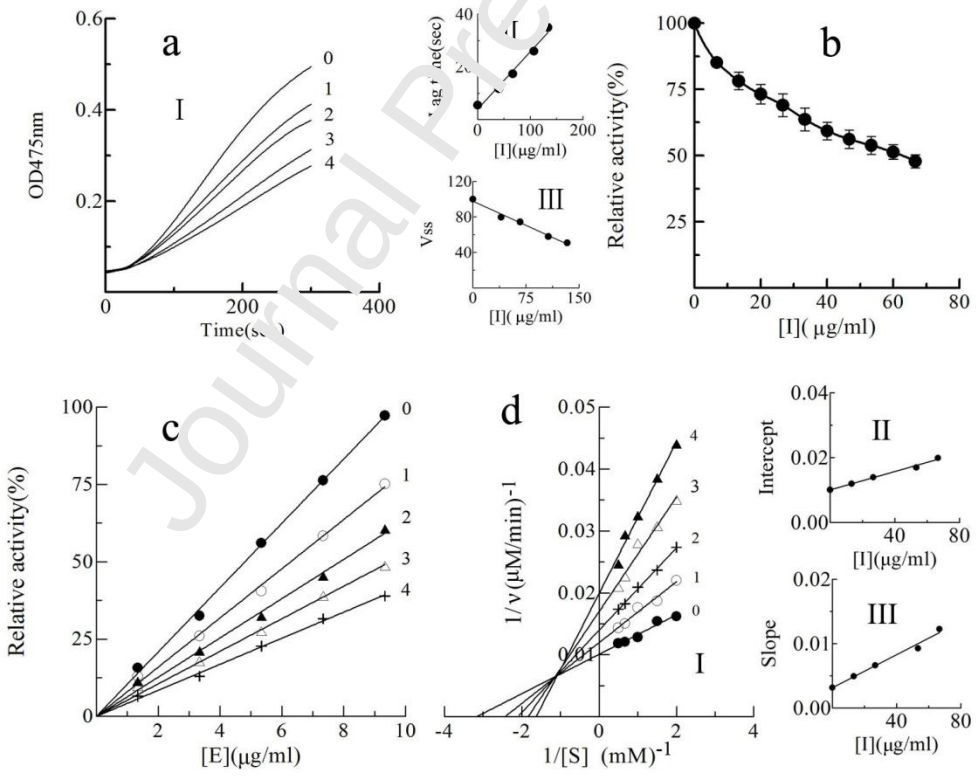

Figure 2. Determination of the inhibitory effects of CT on the monophenolase and diphenolase activity of mushroom tyrosinase. (a) Inhibitory activity of the CT on monophenolase activity of mushroom tyrosinase. (I) Progress curve for the oxidation of L-Tyr by the enzyme. The concentrations of the inhibitor for curves 0-4 are 0, 40, 66.67, 106.67, and 133.33 μg/mL. (II) Effects of condensed tannins on the lag time of mushroom tyrosinase. (III) Effects of condensed tannins or the steady-state rate of monophenolase; Vss represented the steady-state rate of monophenolase. (b) Inhibitory activity of the condensed tannins on diphenolase activity of mushroom tyrosinase. (c-d) Determination of the inhibitory mechanism (c) and type (d) of condensed tannins extracted from the fruit of Sour jujube. L-dopa was used as the substrate to detect the inhibition type and mechanism of of tyrosinase diphenolase. (I) Lineweaver-Burk plots for diphenolase activity. (II) The plot of slope versus the concentration of the condensed tannins for determining the inhibition constants KI. (III) The plot of intercept versus the concentration of the condensed tannins for determining the inhibition constants KIS. 0-4 represents the concentrations of the condensed tannins, which were 0, 13.33, 26.67, and 53.33, 66.67 μg/mL.

3.4 Hydroxylation of L-Lyr and Oxidation of L-DOPA influenced by the Presence of CT

To further confirm that CT from the fruit of Sour jujube interfered with the hydroxylation of L-Lyr by tyrosinase, spectra were obtained during the oxidation of L-Tyr in the absence and presence of CT (100 μg/mL). We found that a series of absorption peaks appear at 475 nm when CT is not added. However, in the presence of CT, the intensity of the peak gradually decreased (Fig.3 b).

The oxidization of L-DOPA by $NaIO_4$ in the absence and presence of the CT was also investigated. As shown in Fig. 3 c, there were no characteristic peaks without $NaIO_4$; Conversely, a characteristic peak appeared at 475 nm while NaIO4 was involved. However, the intensity of the peak shows an obvious decrease with the addition of varying concentrations of CT (50 and 100 μg/mL).

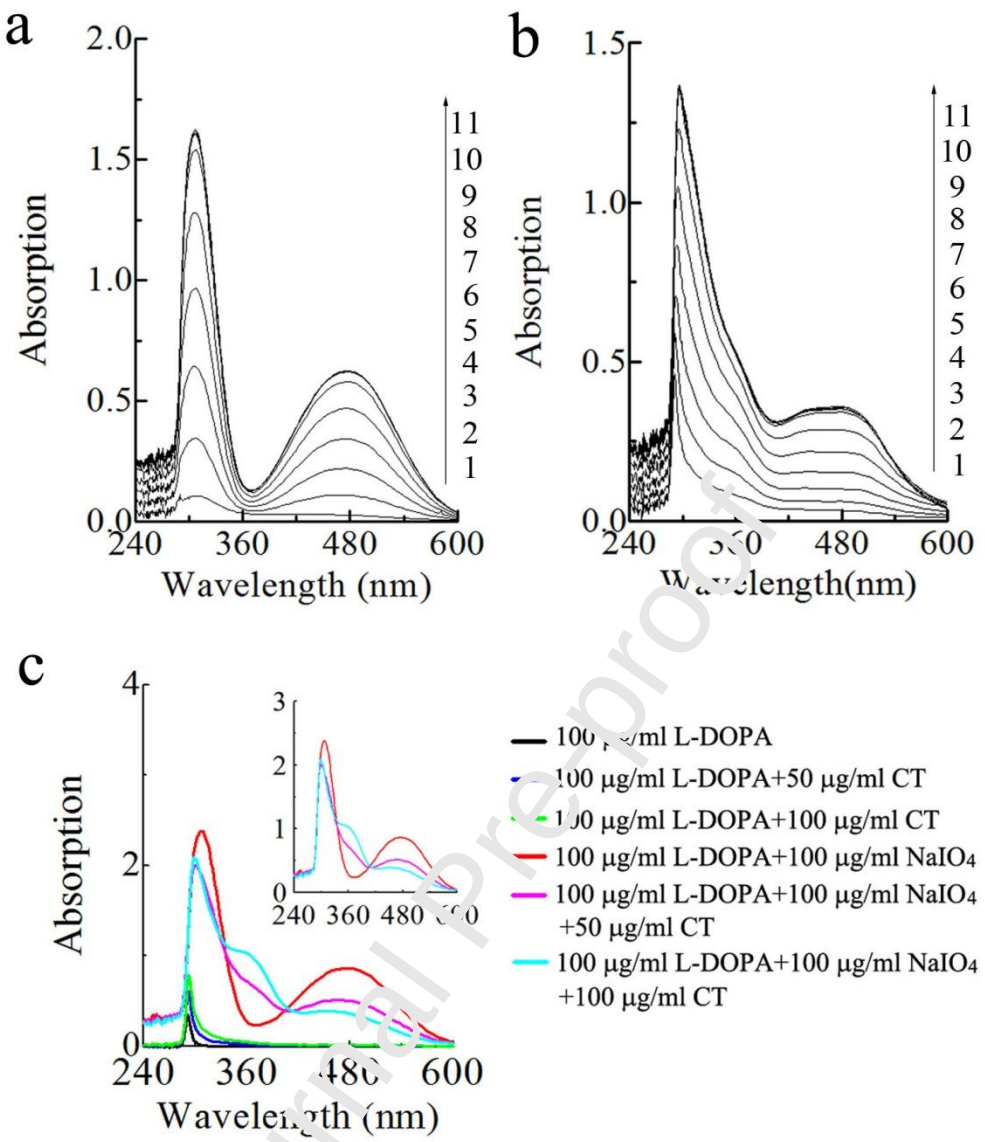

Figure 3. The change in the spectra obtained during the oxidation of L-Tyr and L-DOPA with the CT by mushroom tyrosinase. (a-b) The oxidation of L-Tyr absence and presence of CT (100 μg/mL) respectively (c) UV-Vis spectra for the oxidation of L-DOPA. The assay was performed in 3 ml of 50 mM sodium phosphate buffer (pH 6.8) at 30℃.

3.5 The Chelating Ability between Cu2+ and CT

In this study, the direct interaction between CT and copper ions was detected by full wavelength scanning (240-600 nm). The results showed that with the increase of copper ion concentration, the interaction of CT with copper ions appeared as a slight redshift phenomenon (Fig. 4), suggesting that CT had good copper ion reduction ability and metal chelation ability on the enzyme.

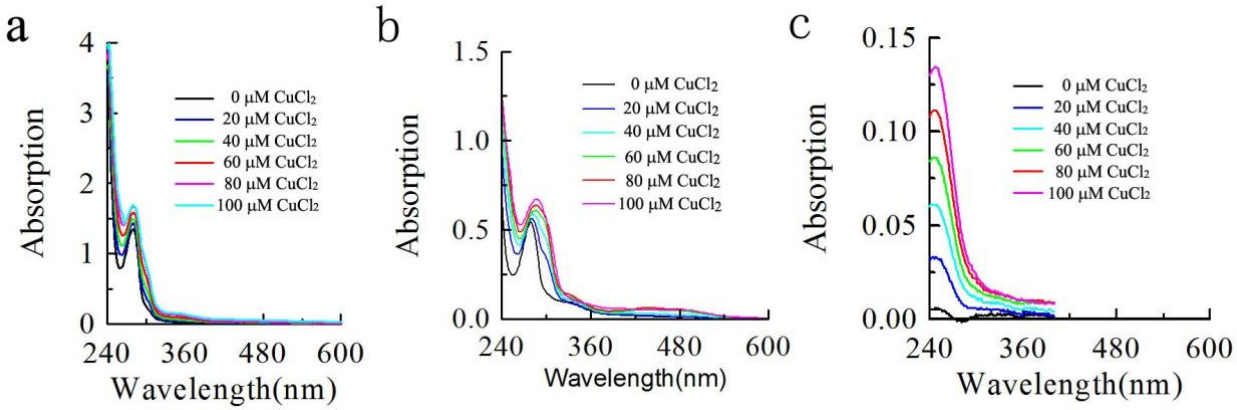

Fig. 4 The metal chelating ability of CT . The concentration of CT is 100 μg/mL. a, b, and c represented CT, catechin (positive control), and PBS (negative control).

3.6 Analysis of fluorescence intensity change

As shown in Fig. 5 a, an obvious peak appeared at 337 nm with an excitation of 290 nm. As the CT concentration increased, the fluorescence intensity of tyrosinase weakened significantly (Fig. 5 c). However, there was no significant red shift appeared (Fig. 5 b). A good linear is obtained by Stern-Volmer plot in Fig. 5 d, which could calculate the quenching constant（Kq）and the Stern–Volmer quenching constant（Ksv）values of 3.35×10^{13} $LM^{-1}s^{-1}$ and 3.35×10^{3} M^{-1}, respectively. The Kq value is much higher than 2.0×10^{10} L Mol $^{-1}$ s^{-1}, so the quenching process is a static quenching process.

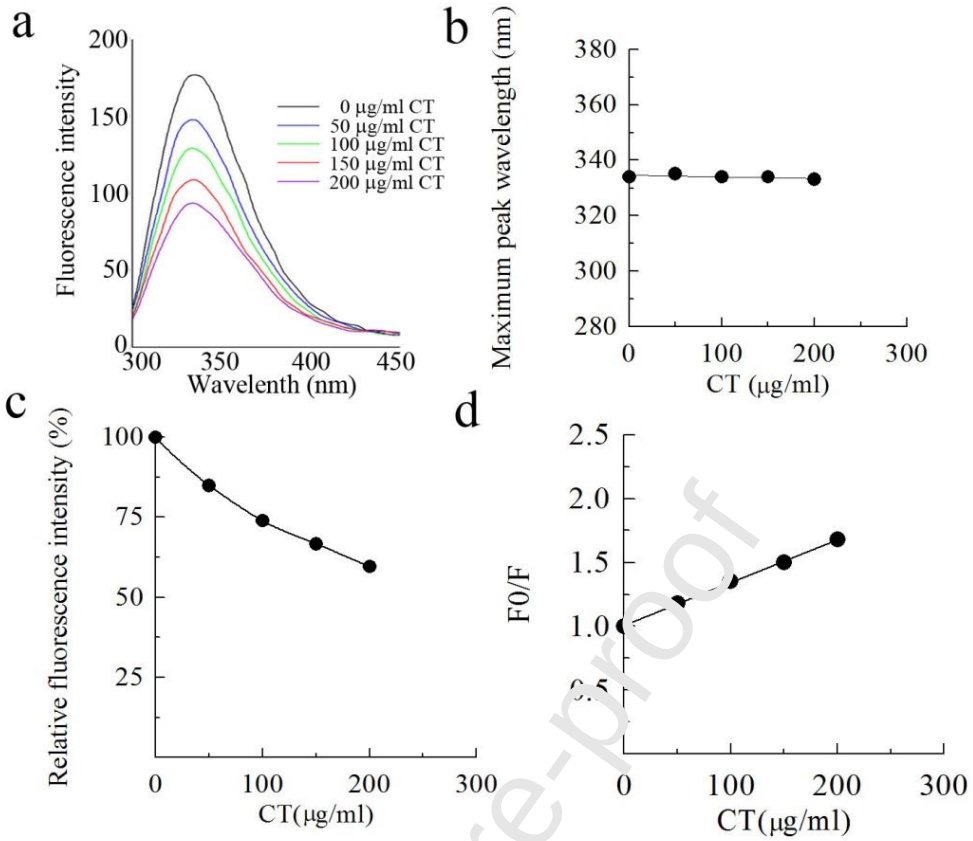

Figure 5. Changes in tyrosinase intrinsic fluorescence. (a) Fluorescence emission spectra of mushroom tyrosinase in the presence of CT with different concentrations. (b) Maximum florescence intensity changes (%); (c) Relative florescence intensity changes; (d) the Stern–Volmer plot for the fluorescence quenching of tyrosinase. F_0 and F are the fluorescence intensities before and after the addition of the CT.

3.7 Molecular docking

The protein crystal structure was optimized and the ligand was connected to the target active cavity. The binding force was analyzed according to the docking results, as shown in Fig. 6. L-Tyr, L-Dopa, catechin (monomers of the CT) and target (tyrosinase) were selected for the docking simulation to detect the binding of small molecular ligands to the target active sites. The energy scores of the most stable docking models for L-Tyr, L-dopa, catechin and catechin trimer were - 11.43, - 14.39, - 18.48, - 22.59 kcal / mol, respectively.

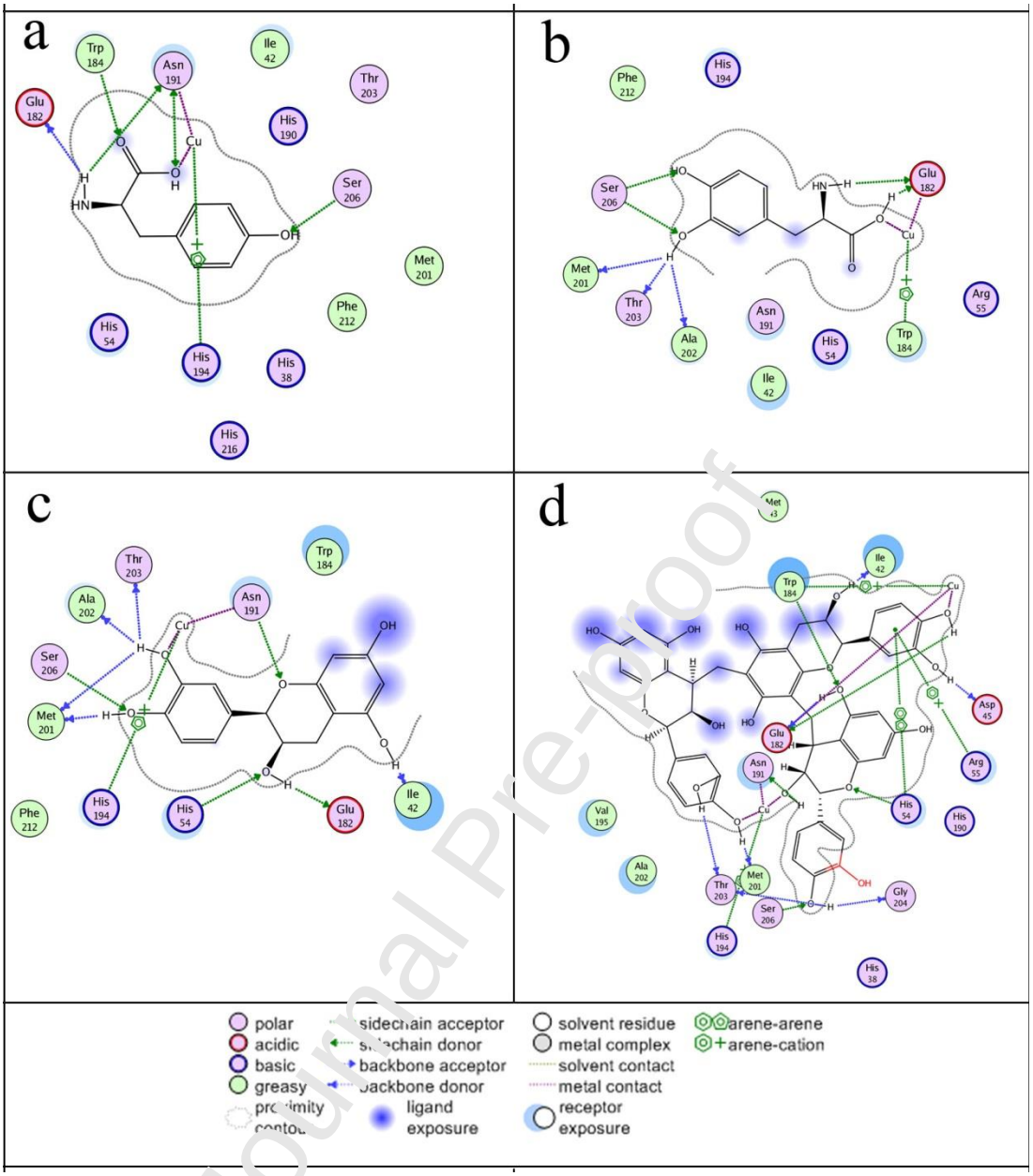

Figure 6. Molecular dock between condensed tannins and mushroom tyrosinase. L-Tyr (a), L-Dopa (b), catechin (c), catechin trimer (d).

The molecular docking results showed that the ligands could also chelate the copper ions in the enzyme active site(Fig. 6). Furthermore, the hydroxyl radical and the benzene ring structure in the structure of the catechin ligand were the key factors for the interaction between ligands and protein. Among them, the 3 position hydroxyl attached to hydroxylphenyl formed H-bonds with Thr203, Ala202 and Met201; the 4 position hydroxyl formed hydrogen bonds with Met201; the 3 position hydroxyl in benzopyran formed H-bonds with Glu182, as well as the 5 position hydroxyl with Ile42; oxygen and hydroxyl oxygen connected to the benzopyran skeleton formed weak electrostatic

interactions with Asn191 and His54; formed a π-π stacking interaction between His194 and benzene in ligands. In addition, the catechin ligands can be well placed within the hydrophobic pocket consisting of Asn191, Thr203, Ala202, Ser206, Met201, His194, His54, Glu182 and Ile42, to realize the strong interaction between protein and ligand.

4. Discussion

Tyrosinase is a copper oxidase that has three states of tyrosinase, including oxidation, reduction and deoxidization. It is a key enzyme in the synthesis of melanin, which catalyzes the hydroxylation of monophenol to catechol, which is then oxidized to DOPA[1, 31].This study reported the inhibitory effect of CT from the fruit of Sour jujubeon both monophenolic dehydrogenase and biphenol oxygenase activity of tyrosinase. Regarding monophenolase activity, CT can effectively reduce the monophenolase steady-state activity remarkable in a dose-dependent manner,with changing the lag time (Fig. 2). The presence of o-diphenol in the monophenolase reaction system shortens the lag time, because the lag time is the time required to reach the steady o-diphenol concentration. For diphenolase activity, types of tyrosinase inhibition mechanisms under the presence of CT from the fruit of Sour jujube was reversible suggesting that CT just reduced the speed of the enzymatic reaction, but did not affect the occurrence of the reaction. The concentration of inhibitors leading to the half activity of the enzyme was 57.67 μg/mL suggesting that CT from the fruit of Sour jujube had a strong tyrosinase-inhibiting activity, the several studies showed methanol extracts from sorghum distillery residue [32], ergothioneine [33] and arbutin[34] all can inhibit tyrosinase activity, with IC 50 were 580 μg/mL, 1025 μg/mL, 462.4 μg/mL respectively. Obviously, CT from the fruit of Sour jujube had better tyrosinase inhibition ability than some inhibitors in the previous studies.

Further investigated the kinetic mechanism showed that the CT changed the maximum reaction rate of the enzymatic reaction velocity (Vm) and Michaelis constant (Km) and was a mix type inhibitor. As shown in Fig. 4b, a group of slope intercept changes but intersects in the two quadrants, which indicates that Km increases with the increase of concentration, and Vm decreases with the increase of concentration, which is a mixed competitive inhibition. The results show that the CT not only competes with the substrate for the active site of enzyme, but also binds to the enzyme substrate

complex. It is indicating that CT affected not only the affinity of the enzyme for the substrate, but also the ability of enzyme catalysis. This mode of the inhibitory mechanism also appeared in many other tyrosinase inhibitors from plants[35-38]. Furthermore, KI< KIS indicating that the binding capacity of inhibitors to free enzymes was much stronger than binding to the enzyme-substrate complex[39].

After we knew inhibition type and kinetic mechanism of CT from the fruit of Sour jujube on tyrosinase activity, however, what is its specific molecular mechanism? So the UV scanning, o-quinone interaction, copper chelating, fluorescence quenching, and molecular docking assays were to further unravel and confirm the molecular mechanism of anti-tyrosinase by CT.

Tyrosinase has a unique dual catalytic function. Firstly, it catalyzes the hydroxylation of L-tyrosine to form L-dopa, then oxidizes L-dopa to form DOPA quinone, and finally forms melanin[40]. UV scanning and o-quinone interaction assay showed that hydroxylation of L-Lyr and oxidation of L-DOPA influenced by the Presence of CT. Particularly, L-DOPA alone did not show any characteristic peaks, while the oxidation of L-DOPA by $NaIO_4$ gave rises to the corresponding o-quinones with a characteristic peak at 475 nm, the peak value was negatively correlated with the concentration of CT. It revealed that CT inhibits tyrosinase activity by not only disturbing the formation of L-DOPA, but also reducing o-quinone generation. It suggests that the inhibition of CT on the double catalysis of tyrosinase is omnidirectional.

Most of the tyrosinase inhibitors have the same characteristics of binding copper ions in the active center of the enzyme, for instance, kojic acid and chalcones. Moreover, it is reported that CT has chelated metal ions[41-43], and the two copper ions are within the active site of tyrosinase. Thus, we asked if the inhibition mechanism of CT involves interacting with copper ions of the enzyme. The copper chelating assay performed to confirm the direct interaction between CT copper ions. The results indicated CT alters the conformation of tyrosinase by form a CT-copper complex, which may be one of the main reasons for CT inhibition of tyrosinase activity.

The hydroxyl groups of CT have a critical effect on tyrosinase activity[44, 45]. Through HPLC and MALDI analysis, we found that CT from Sour jujube fruit is mainly composed of catechin and epicatechin containing two hydroxyl groups, which

may be one of the important reasons for the inhibition of tyrosinase by CT. Several types of researches showed fluorescence quenching assay often used in the interaction between protein and small molecules. With the CT concentration increased, the fluorescence intensity of tyrosinase weakened significantly indicating that the quencher interacted with the fluorophore. However, there was no apparent blueshift phenomenon appeared in the maximum emission spectra of tyrosinase in the presence of CT. Therefore, the combination of tyrosinase and CT only affected the fluorophore microenvironment of the tyrosinase, but not changed the direction and structure of the tyrosinase.

To further explain inhibitory mechanism between CT with mushroom tyrosinase, MOE2010 was adopted to stimulated the tyrosinase with L-Tyr, L-DOPA, catechin, and trimer of catechin. The docking simulation revealed that the L-DOPA, catechin and trimer of catechin could chelate the copper ions in the enzyme active site, whereas L-Tyr could not chelate the copper ions. These results were supported the detection result of copper chelating capacity. Additionally, there are six relatively conserved histidine residues within the active site of tyrosinase, each of the three subunits is complexed with one copper ion to form a coordination structure of binuclear copper as the auxiliary group. In contrast, the two copper ions are connected by oxygen bridges[46-48]. Because of the formation of the van der Waals force, the hydrophobic and hydrogen bonding interactions between ligand compounds, and the amino acid residues around the target protein receptor pockets, the ligand compounds can be closely integrated with the target protein. It is also possible that the presence of these forces enables compounds to exert their biological activity. The amino acids in tyrosinase forming interaction with catechin ligands were Asn191, Thr203, Ala202, Ser206, Met201, His194, His54, Glu182 and Ile42. The molecular docking results well support the mixed inhibition type we observed, because this inhibition type generally appeared when the inhibitor has multiple possible binding sites. The model of molecular docking and corresponding inhibition mechanism was also found in those reported in hot spots[42, 43, 49]. Therefore, the molecular docking model of tyrosinase with CT was credible and could be valid and feasible for screening and identification of more lead complexes of tyrosinase inhibitors.

5. Conclusion

In conclusion, the CT from the Sour jujube fruit displayed efficient both monophenolase and diphenolase inhibitory activities of tyrosinase. The inhibitory mechanism by which the CT inhibits tyrosinase may be through binding to the specific amino acid residues or to the copper ion of the active site of tyrosinase, which are two ways to disperse the acylation of L-Try and the oxidation of L-Dopa, ultimately affect the synthesis of melanin. Therefore, The sour jujube fruit is a potential natural source of tyrosinase inhibitors, and has the potential to be used in food preservation, whitening cosmetics, and so on. This research contributed to better understand the inhibition mechanism of tyrosinase inhibitors by the interaction between tyrosinase and the inhibitors.

Funding: This work was supported by grants from the the Science and Technology Research Project from Hubei Provincial Education Department (D20191301), National Nature Science Foundation of China Grant (No. 81402309), the Key scientific research projects of colleges and universities in Henan Province (No. 21A180003) and Henan University of Urban Construction Academic technology leader program（xs2019006-HY）.

Author Contributions: Data curation, Wei Song; Formal analysis, Yuan-Jing Ren; Funding acquisition, Wei Song and Hai-Bo Yang; Investigation, Wei Song and Yuan-Jing Ren; Project administration, Lu-Lu Liu, Shu-Dong Wei and Hai-Bo Yang; Resources, Lu-Lu Liu; Supervision, Shu-Dong Wei and Hai-Bo Yang; Writing – original draft, Wei Song; Writing – review & editing, Hai-Bo Yang.

Conflicts of Interest: The authors declare no conflicts of interest.

Abbreviations:

CT	soluble condensed tannin
Sour jujube	*Ziziphus jujuba Mill. var. spinosa (Bunge) Hu ex H. F. Chow*
KI	inhibition constant
KIS	inhibition constant
NaIO4	Sodium periodate
HPLC-ESI-MS	high performance liquid chromatography electrospray ionization mass spectrometry
GC/EGC	gallate catechin/epigallate catechin
C/EC	catechin/epicatechin
Kq	the quenching constant
Ksv	the Stern–Volmer quenching constant

References

[1] P.A. Riley, Mechanistic aspects of the control of tyrosinase activity, Pigment Cell Res 6(4 Pt 1)

(1993) 182-5.

[2] H.W. Ryu, S.H. Jeong, M.J. Curtis-Long, S. Jung, J.W. Lee, H.S. Woo, J.K. Cho, K.H. Park, Inhibition effects of mangosenone F from Garcinia mangostana on melanin formation in B16F10 cells, J Agric Food Chem 60(34) (2012) 8372-8.

[3] S.H. Lee, K. Baek, J.E. Lee, B.G. Kim, Using tyrosinase as a monophenol monooxygenase: A combined strategy for effective inhibition of melanin formation, Biotechnol Bioeng 113(4) (2016) 735-43.

[4] F. Moradi, R.D.E. Sewell, Z. Lorigooini, M. Rafieian-Kopaei, Immunosuppression-lipid Metabolism Interplay and Medicinal Plants in Atherosclerosis: A Review, Curr Pharm Des 24(24) (2018) 2789-2793.

[5] S. Sultana, H.M. Asif, Review: Medicinal plants combating against hypertension: A green antihypertensive approach, Pak J Pharm Sci 30(6) (2017) 2311-2319.

[6] M. Bose, M. Kamra, R. Mullick, S. Bhattacharya, S. Das, A.A. Karande, Identification of a flavonoid isolated from plum (Prunus domestica) as a potent inhibitor of Hepatitis C virus entry, Sci Rep 7(1) (2017) 3965.

[7] A.H. Ahmed, M. Ejo, T. Feyera, D. Regassa, B. Mummed, S.A. Huluka, In Vitro Anthelmintic Activity of Crude Extracts of Artemisia herba-alba and Punica granatum against Haemonchus contortus, J Parasitol Res 2020 (2020) 4950196.

[8] H.Y. Ahn, J.-H. Cho, D. Nam, E.-J. Kim, I.-H. Ha, Efficacy and safety of Cortex Eucommiae (Eucommia ulmoides Oliver) extract in subjects with mild osteoarthritis: Study protocol for a 12-week, multicenter, randomized, double-blind, placebo-controlled trial, Medicine 98 (2019).

[9] L. Song, L. Zhang, L. Xu, Y. Ma, W. Liu, Y. Liu, Y. Wang, Optimized Extraction of Total Triterpenoids from Jujube (Ziziphus jujuba Mill.) and Comprehensive Analysis of Triterpenic Acids in Different Cultivars, Plants (Basel) 9(4) (2020).

[10] C. Guo, J. Wu, H. He, H. Liu, Y. Wang, N. Wei, C. Wang, W. Lin, H. Su, Evaluation of the medical economics and safety: two methods for the endoscopic removal of jujube pits, Rev Esp Enferm Dig 111(3) (2019) 209-213.

[11] S.H. Choi, J.B. Ahn, N. Kozukue, C.E. Levin, M. Friedman, Distribution of free amino acids, flavonoids, total phenolics, and antioxidative activities of Jujube (Ziziphus jujuba) fruits and seeds harvested from plants grown in Korea, J Agric Food Chem 59(12) (2011) 6594-604.

[12] Z. Wu, H. Li, Y. Wang, D. Yang, H. Tan, Y. Zhan, Y. Yang, Y. Luo, G. Chen, Optimization extraction, structural features and antitumor activity of polysaccharides from Z. jujuba cv. Ruoqiangzao seeds, Int J Biol Macromol 135 (2019) 1151-1161.

[13] P. Song, Y. Zhang, G. Ma, A. Zhou, J. Xie, Gastrointestinal Absorption and Metabolic Dynamics of Jujuboside A, A Saponin Derived from the Seed of Ziziphus jujuba, J Agric Food Chem 65(38) (2017) 8331-8339.

[14] H.J. Park, I.H. Jung, H. Kwon, J. Yu, E. Jo, H. Kim, S.J. Park, Y.C. Lee, D.H. Kim, J.H. Ryu, The ethanol extract of Zizyphus jujuba var. spinosa seeds ameliorates the memory deficits in Alzheimer's disease model mice, J Ethnopharmacol 233 (2019) 73-79.

[15] S. Guo, J.A. Duan, Y. Li, R. Wang, H. Yan, D. Qian, Y. Tang, S. Su, Comparison of the Bioactive Components in Two Seeds of Ziziphus Species by Different Analytical Approaches Combined with Chemometrics, Front Pharmacol 8 (2017) 609.

[16] S.Y. Jo, I.H. Jung, J.H. Yi, T.J. Choi, S. Lee, J.W. Jung, J. Yun, Y.C. Lee, J.H. Ryu, D.H. Kim, Ethanol extract of the seed of Zizyphus jujuba var. spinosa potentiates hippocampal synaptic

transmission through mitogen-activated protein kinase, adenylyl cyclase, and protein kinase A pathways, J Ethnopharmacol 200 (2017) 16-21.

[17] M. Li, Y. Wang, B. Tsoi, X.J. Jin, R.R. He, X.J. Yao, Y. Dai, H. Kurihara, X.S. Yao, Indoleacetic acid derivatives from the seeds of Ziziphus jujuba var. spinosa, Fitoterapia 99 (2014) 48-55.

[18] M. Zeyadi, Y.Q. Almulaiky, A novel peroxidase from Ziziphus jujuba fruit: purification, thermodynamics and biochemical characterization properties, Sci Rep 10(1) (2020) 8007.

[19] S.P. Engozogho Anris, A.B. Bi Athomo, R. Safou Tchiama, F.J. Santiago-Medina, T. Cabaret, A. Pizzi, B. Charrier, The condensed tannins of Okoume (Aucoumea klaineana Pierre): A molecular structure and thermal stability study, Sci Rep 10(1) (2020) 1773.

[20] K. Peng, Q. Huang, Z. Xu, T.A. McAllister, S. Acharya, I. Mueller-Harvey, C. Drake, J. Cao, Y. Huang, Y. Sun, S. Wang, Y. Wang, Characterization of Condensed Tannins from Purple Prairie Clover (Dalea purpurea Vent.) Conserved as either Freeze-Dried Forage, Sun-Cured Hay or Silage, Molecules 23(3) (2018).

[21] Chai, Wei-Ming, Huang, Qian, Lin, Mei-Zhen, Ou-Yang, Chong, Wen-Yang, Wang, Condensed Tannins from Longan Bark as Inhibitor of Tyrosinase: Structure, Activity, and Mechanism, Journal of agricultural and food chemistry (2018).

[22] G.S. Castaneda-Ramirez, J.F.J. Torres-Acosta, C.A. Sandoval-Castro, P.G. Gonzalez-Pech, V.P. Parra-Tabla, C. Mathieu, Is there a negative association between the content of condensed tannins, total phenols, and total tannins of tropical plant extracts and in vitro anthelmintic activity against Haemonchus contortus eggs?, Parasitol Res 116(12) (2017) 3341-3348.

[23] C.G. Kato, G.A. Goncalves, R.A. Peralta, F.V. Seixas, A.B. de Sa-Nakanishi, L. Bracht, J.F. Comar, A. Bracht, R.M. Peralta, Inhibition of alpha-Amylases by Condensed and Hydrolysable Tannins: Focus on Kinetics and Hypoglycemic Actions, Enzyme Res 2017 (2017) 5724902.

[24] K. Nokihara, A. Hirata, T. Sogon, T. Ohyama, Preparative scale isolation, purification and derivatization of mimosine, a non-proteinogenic amino acid, Amino Acids 43(1) (2012) 475-82.

[25] X. Liang, Y.P. Wu, J.H. Qiu, K. Zhong, H. Gao, A potent antibrowning agent from pine needles of Cedrus deodara: 2R,3R-dihydromyricetin, J Food Sci 79(9) (2014) C1643-8.

[26] S.H. Nile, A. Nile, J. Liu, D.R. Kim, G. Kai, Exploitation of apple pomace towards extraction of triterpenic acids, antioxidant potential, cytotoxic effects, and inhibition of clinically important enzymes, Food Chem Toxicol 131 (2019) 110563.

[27] S. Sut, G. Zengin, F. Maggi, M. Malagoli, S. Dall'Acqua, Triterpene Acid and Phenolics from Ancient Apples of Friuli Venezia Giulia as Nutraceutical Ingredients: LC-MS Study and In Vitro Activities, Molecules 24(6) (2019).

[28] N. Li, Z. Lin, W. Chen, Y. Zheng, Y. Ming, Z. Zheng, W. Huang, L. Chen, J. Xiao, H. Lin, Corilagin from longan seed: Identification, quantification, and synergistic cytotoxicity on SKOv3ip and hey cells with ginsenoside Rh2 and 5-fluorouracil, Food Chem Toxicol 119 (2018) 133-140.

[29] T.S. Chang, An updated review of tyrosinase inhibitors, Int J Mol Sci 10(6) (2009) 2440-75.

[30] W. Song, X.F. Zhu, X.D. Ding, H.B. Yang, S.T. Qin, H. Chen, S.D. Wei, Structural Features, Antioxidant and Tyrosinase Inhibitory Activities of Proanthocyanidins in Leaves of Two Tea Cultivars, International Journal of Food Properties (2016).

[31] M. Sugumaran, A caution about the azide inhibition of enzymes associated with electrophilic metabolites, Biochem Biophys Res Commun 212(3) (1995) 834-9.

[32] C.Y. Wang, C.C. Ng, H.T. Lin, Y.T. Shyu, Free radical-scavenging and tyrosinase-inhibiting activities of extracts from sorghum distillery residue, J Biosci Bioeng 111(5) (2011) 554-6.

[33] W.C. Liao, H.W. Wen, P.C. Tsai, H.F. Wang, Y.H. Liu, C.F. Chan, Kinetics of Ergothioneine Inhibition of Mushroom Tyrosinase, Applied Biochemistry & Biotechnology 166(2) (2012) 259-267.

[34] M. Tada, M. Kohno, Y. Niwano, Alleviation effect of arbutin on oxidative stress generated through tyrosinase reaction with L-tyrosine and L-DOPA, BMC Biochem 15 (2014) 23.

[35] J. Cabanes, F. Garcia-Carmona, F. Garcia-Canovas, J.L. Iborra, J.A. Lozano, Kinetic study on the slow inhibition of epidermis tyrosinase by m-coumaric acid, Biochim Biophys Acta 790(2) (1984) 101-7.

[36] L. Zhang, X. Zhao, G.J. Tao, J. Chen, Z.P. Zheng, Investigating the inhibitory activity and mechanism differences between norartocarpetin and luteolin for tyrosinase: A combinatory kinetic study and computational simulation analysis, Food Chem 223 (2017) 40-48.

[37] Y.J. Zhu, L. Qiu, J.J. Zhou, H.Y. Guo, Y.H. Hu, Z.C. Li, Q. Wang, Q.X. Chen, B. Liu, Inhibitory effects of hinokitiol on tyrosinase activity and melanin biosynthesis and its antimicrobial activities, J Enzyme Inhib Med Chem 25(6) (2010) 798-803.

[38] L.P. Xie, Q.X. Chen, H. Huang, H.Z. Wang, R.Q. Zhang, Inhibitory effects of some flavonoids on the activity of mushroom tyrosinase, Biochemistry (Mosc) 68(4) (2003) 487-91.

[39] Z. Ashraf, M. Rafiq, H. Nadeem, M. Hassan, S. Afzal, M. Waseem, K. Afzal, J. Latip, Carvacrol derivatives as mushroom tyrosinase inhibitors; synthesis, kinetic mechanism and molecular docking studies, PLoS One 12(5) (2017) e0178069.

[40] S. Ito, K. Wakamatsu, H. Ozeki, Chemical analysis of melanins and its application to the study of the regulation of melanogenesis, Pigment Cell Res 13 Suppl 8 (2000) 103-9.

[41] E. Akyilmaz, E. Yorganci, E. Asav, Do copper ions activate tyrosinase enzyme? A biosensor model for the solution, Bioelectrochemistry 78(2) (2010) 155-60.

[42] H.C. Kwong, C.S. Chidan Kumar, S.H. Mah, T.S. Chia, C.K. Quah, Z.H. Loh, S. Chandraju, G.K. Lim, Novel biphenyl ester derivatives as tyrosinase inhibitors: Synthesis, crystallographic, spectral analysis and molecular docking studies, PLoS One 12(2) (2017) e0170117.

[43] L. Gou, J. Lee, H. Hao, Y.D. Park, Y. Zhan, Z.R. Lu, The effect of oxaloacetic acid on tyrosinase activity and structure: Integration of inhibition kinetics with docking simulation, Int J Biol Macromol 101 (2017) 59-66.

[44] W.M. Chai, M.Z. Lin, Y.X. Wang, K.L. Xu, W.Y. Huang, D.D. Pan, Z.R. Zou, Y.Y. Peng, Inhibition of tyrosinase by cherimoya pericarp proanthocyanidins: Structural characterization, inhibitory activity and mechanism, Food Res Int 100(Pt 1) (2017) 731-739.

[45] W.M. Chai, M.K. Wei, R. Wang, R.G. Deng, Z.R. Zou, Y.Y. Peng, Avocado Proanthocyanidins as a Source of Tyrosinase Inhibitors: Structure Characterization, Inhibitory Activity, and Mechanism, J Agric Food Chem 63(33) (2015) 7381-7.

[46] R. Biswas, J. Chanda, A. Kar, P.K. Mukherjee, Tyrosinase inhibitory mechanism of betulinic acid from Dillenia indica, Food Chem 232 (2017) 689-696.

[47] E.M. Brasil, L.M. Canavieira, E.T.C. Cardoso, E.O. Silva, J. Lameira, J.L.M. Nascimento, V.L. Eifler-Lima, B.M. Macchi, D. Sriram, P.V. Bernhardt, J.R.A. Silva, C.M. Williams, C.N. Alves, Inhibition of tyrosinase by 4H-chromene analogs: Synthesis, kinetic studies, and computational analysis, Chem Biol Drug Des 90(5) (2017) 804-810.

[48] T. Oyama, A. Yoshimori, S. Takahashi, T. Yamamoto, A. Sato, T. Kamiya, H. Abe, T. Abe, S.I. Tanuma, Structural insight into the active site of mushroom tyrosinase using phenylbenzoic acid derivatives, Bioorg Med Chem Lett 27(13) (2017) 2868-2872.

[49] H.C. Tang, Y.C. Chen, Identification of tyrosinase inhibitors from traditional Chinese medicines

for the management of hyperpigmentation, Springerplus 4 (2015) 184.

Author statement:

Song Wei：Data curation，Funding acquisition，Investigation，Writing – original draft. Ren Yuan-Jing: Formal analysis, Investigation. Liu Lu-Lu: Resources, Project administration. Wei Shu-Dong: Project administration , Writing – review & editing; Yang Hai-Bo: Project administration, Supervision, Funding acquisition , Writing – review & editing

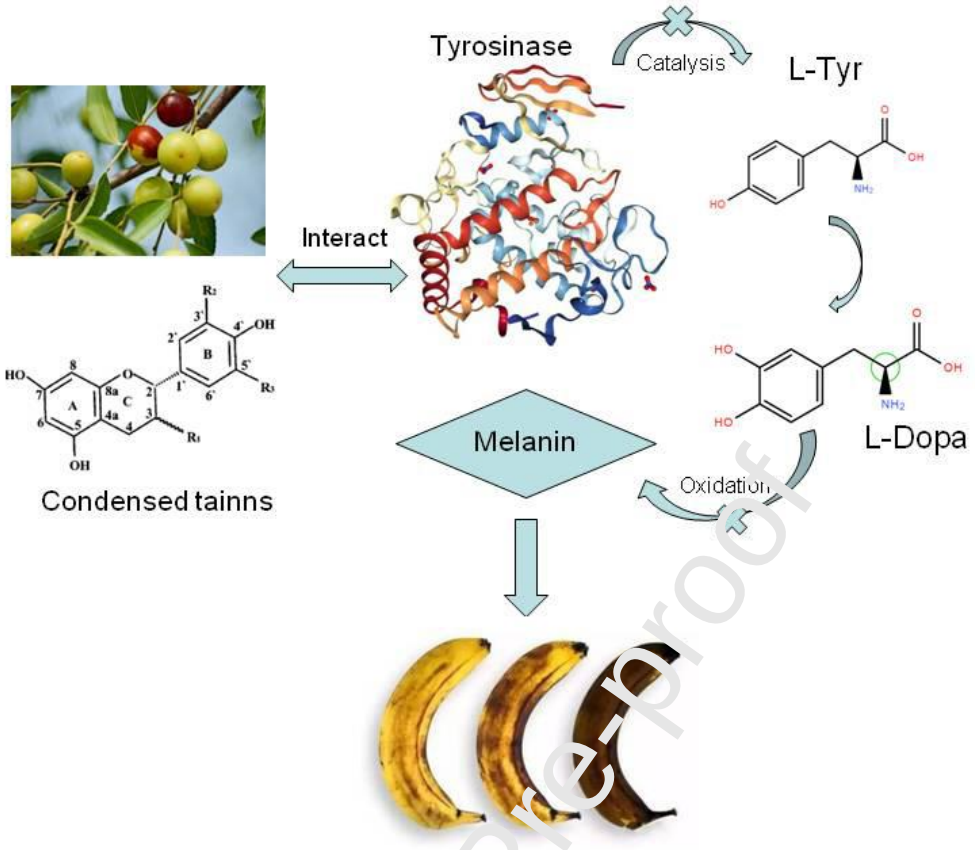

Graphical abstract

CT from the fruit of Sour jujube inhibit the activity of tyrosinase through simultaneous interaction with its copper ions and specific amino acid residues.